Commun Nonlinear Sci Numer Simulat 17 (2012) 4304–4315

Contents lists available at SciVerse ScienceDirect

Commun Nonlinear Sci Numer Simulat

journal homepage: www.elsevier.com/locate/cnsns

Algebraic approach for the exploration of the onset of chaos in discrete nonlinear dynamical systems

Minvydas Ragulskis [a,*], Zenonas Navickas [b,1], Rita Palivonaite [a,2], Mantas Landauskas [a,3]

[a] Research Group for Mathematical and Numerical Analysis of Dynamical Systems, Kaunas University of Technology, Studentu 50-222, Kaunas LT-51368, Lithuania
[b] Department of Applied Mathematics, Kaunas University of Technology, Studentu 50-325, Kaunas LT-51368, Lithuania

ARTICLE INFO

Article history:
Received 9 December 2010
Received in revised form 18 January 2012
Accepted 18 March 2012
Available online 28 March 2012

Keywords:
Hankel matrix
Rank of a sequence
Algebraic decomposition
Onset of chaos

ABSTRACT

An algebraic approach based on the rank of a sequence is proposed for the exploration of the onset of chaos in discrete nonlinear dynamical systems. The rank of the partial solution is identified and a special technique based on Hankel matrices is used to decompose the solution into algebraic primitives comprising roots of the modified characteristic equation. The distribution of roots describes the dynamical complexity of a solution and is used to explore properties of the nonlinear system and the onset of chaos.

1. Introduction

The onset of chaos is a classical research area exploring different physical, mathematical and engineering aspects of nonlinear dynamical systems. The period-doubling onset of chaos is described using formal techniques in [1]. Multifractal scaling structure at the onset of chaos is explored in [2]. The onset of chaos is explored in different nonlinear systems – in differential delay equations [3]; in nuclear states of molecules [4,5]; in the logistic map driven by colored noise [6]. A variety of period-doubling universality classes in multi-parameter analysis of transition to chaos is explored in [7]. Chaotic attractors generated by iterated function systems and the emergence of chaotic behavior are studied in [8]; the cobweb model is used to illustrate the instability and the onset of chaos in [9]. A route to ergodicity breakdown and statistical descriptions of nonlinear systems at the onset of chaos are investigated in [10,11]. Fibonacci order in the period-doubling cascade to chaos and the comparison of recurrence quantification methods for the analysis of temporal and spatial chaos are discussed in [12,13]; the transition from maps to turbulence is discussed in [14]. Applicability of Hamiltonian geometrical criterion for the exploration of chaos determined by the dynamical curvature of a conformal metric for a nonlinear Hamiltonian system is discussed in [15]. A computer-algebraic criterion based on the autocorrelation function and Laplace–Borel transformation for the onset of chaos in nonlinear dynamical systems is proposed in [16].

* Corresponding author. Tel.: +370 69822456; fax: +370 37330446.
E-mail addresses: minvydas.ragulskis@ktu.lt (M. Ragulskis), zenonas.navickas@ktu.lt (Z. Navickas), rita.palivonaite@ktu.lt (R. Palivonaite), mantas.landauskas@ktu.lt (M. Landauskas).
URL: http://www.personalas.ktu.lt/~mragul (M. Ragulskis).
[1] Tel.: +370 68223789.
[2] Tel.: +370 67287255.
[3] Tel.: +370 67713231.

1007-5704/$ - see front matter © 2012 Elsevier B.V. All rights reserved.
http://dx.doi.org/10.1016/j.cnsns.2012.03.017

The object of this paper is to explore the onset of chaos also using a computer–algebraic technique. But the main difference of our approach is that we use Hankel matrix based techniques instead. The concept of H-rank and its applicability for mapping manifolds and exploration of the system's sensitivity to initial conditions is introduced in [17].

This paper presents the adaptation of the H-rank technique for the investigation of the complexity of transient processes occurring in a discrete nonlinear dynamical system as it approaches the chaotic state. Algebraic decomposition of a discrete sequence is introduced in Section 2; the computation of ranks of discrete sequences is discussed in Section 3. Numerical experiments with the logistic map and the Mandelbrot set are performed in Sections 4 and 5; concluding remarks are given in Section 6.

2. Algebraic decomposition of a solution of a discrete map

Let S is an infinite sequence of real or complex numbers:

$$S := \{x_r\}_{r=0}^{+\infty}. \tag{1}$$

A finite subsequence comprising first $2k-1$ elements $(x_0, x_1, x_2, \ldots, x_{2k-3}, x_{2k-2})$ can be rearranged into the Hankel matrix $H^{(k)}$:

$$H^{(k)} := [x_{r+s-2}]_{1\leqslant r,s\leqslant k} = \begin{bmatrix} x_0 & x_1 & \cdots & x_{k-1} \\ x_1 & x_2 & \cdots & x_k \\ & & \cdots & \\ x_{k-1} & x_k & \cdots & x_{2k-2} \end{bmatrix}, \tag{2}$$

where the superscript (k) denotes the order of the Hankel matrix. The Hankel transform of the sequence of matrices $\left\{H^{(k)}\right\}_{k=2}^{+\infty}$ yields a sequence of determinants $\left\{\det(H^{(k)})\right\}_{k=2}^{+\infty} = \left\{d^{(k)}\right\}_{k=2}^{+\infty}$.

The rank of a discrete sequence is defined in [18]. It is such a natural number m that satisfies the following condition (if only the rank exists):

$$d^{(m+n)} = 0 \tag{3}$$

for all $n \in N$; if only $d^{(m)} \neq 0$. We will use the notation:

$$HrS = m. \tag{4}$$

If such a number m does not exist, we will denote that the sequence S does not have a rank: $HrS := +\infty$.

Let us assume that the rank of the sequence S exists: $HrS = m$; $m < +\infty$. Then it is possible to construct the characteristic algebraic equation [18,19]:

$$\begin{vmatrix} x_0 & x_1 & \cdots & x_m \\ x_1 & x_2 & \cdots & x_{m+1} \\ & & \cdots & \\ x_{m-1} & x_m & \cdots & x_{2m-1} \\ 1 & \rho & \cdots & \rho^m \end{vmatrix} = 0 \tag{5}$$

which yields m roots $\{\rho_k\}_{k=1}^{m}$. Let us denote the number of different roots by r and recurrence indexes of each different root by $\{n_k\}_{k=1}^{r}$. It is clear that $\sum_{k=1}^{r} n_k = m$. Then, elements of the sequence S can be expressed as [17,18]:

$$x_n = \sum_{k=1}^{r} \sum_{l=0}^{n_k-1} \mu_{kl} \binom{n}{l} \rho_k^{n-l}; \quad n = 0, 1, 2, \ldots; \tag{6}$$

where coefficients $\mu_{kl} \in C$; $k = 1, 2, \ldots, r$; $l = 0, 1, \ldots, n_k - 1$ can be determined from a system of linear algebraic equations which can be formed from equalities Eq. (6) assuming the expressions of elements $x_{n_1}, x_{n_2}, \ldots, x_{n_m}$ of the sequence S where indexes of these elements satisfy inequalities $0 \leqslant n_1 < n_2 < \cdots < n_m < +\infty$. Moreover, such system of linear algebraic equations has one and only solution because its system matrix is a generalized Vandermonde matrix [18]. The subsequence $(x_0, x_1, x_2, \ldots, x_{2k-3}, x_{2k-2})$ is then called the base fragment of the sequence S.

If all roots are different, Eq. (6) reduces to:

$$x_n = \sum_{k=1}^{m} \mu_{k0} \rho_k^n; \quad n = 0, 1, 2, \ldots. \tag{7}$$

Algebraic progressions generalize arithmetic progressions, geometric progressions and provide an insight into the dynamical process governing the evolution of the discrete sequence.

It can be noted that a chaotic sequence does not have a rank. Otherwise it would be an algebraic progression and it could be decomposed into an algebraic form comprising roots and coefficients according to Eq. (6). The dynamics of the sequence would be deterministic, what contradicts to the definition of a chaotic sequence. It should be noted that this conclusion does not contradict to the definition of the deterministic chaos [20]. In general, a sequence has a rank if and only if every element of that sequence corresponds to the value of a function $\sum_{k=1}^{m} Q_k(x)\exp(\lambda_k x)$ on a regular grid, where $Q_k(x)$ are polynomials of x [18]. Thus, for example, the rank of a quasi-periodic sequence $\{\sin(\sqrt{2}(x_0+hj))+\cos(x_0+hj)\}_{j=0}^{+\infty}$ $(x_0, h \in \mathbf{R})$ is equal to 4 (readers are encouraged to check this statement themselves). But a chaotic sequence cannot be decomposed into a finite number of algebraic primitives (the attractor of the corresponding dynamical system would be not strange then).

Example 1 (*All different roots*). Let us consider a periodic sequence $S = (1,0,4,1,0,4,\ldots)$. It is clear that $HrS = 3$ because $d^{(3)} \neq 0$ but

$$d^{(4)} = \begin{vmatrix} 1 & 0 & 4 & 1 \\ 0 & 4 & 1 & 0 \\ 4 & 1 & 0 & 4 \\ 1 & 0 & 4 & 1 \end{vmatrix} = 0$$

and $d^{(4+n)} = 0$ for all $n \in N$. The characteristic algebraic equation

$$\begin{vmatrix} 1 & 0 & 4 & 1 \\ 0 & 4 & 1 & 0 \\ 4 & 1 & 0 & 4 \\ 1 & \rho & \rho^2 & \rho^3 \end{vmatrix} = 65(1-\rho^3) = 0$$

yields roots $\rho_1 = 1$; $\rho_2 = -\frac{1}{2} + i\frac{\sqrt{3}}{2}$; $\rho_3 = -\frac{1}{2} - i\frac{\sqrt{3}}{2}$. All roots are different, thus the linear algebraic system for the identification of coefficients $\{\mu_{k0}\}_{k=1}^{3}$ takes the form:

$$\begin{bmatrix} 1 & 1 & 1 \\ \rho_1 & \rho_2 & \rho_3 \\ \rho_1^2 & \rho_2^2 & \rho_3^2 \end{bmatrix} \begin{bmatrix} \mu_{10} \\ \mu_{20} \\ \mu_{30} \end{bmatrix} = \begin{bmatrix} 1 \\ 0 \\ 4 \end{bmatrix}.$$

Solutions read: $\mu_{10} = \frac{5}{3}$; $\mu_{20} = -\frac{1}{3} + i\frac{2}{\sqrt{3}}$; $\mu_{30} = -\frac{1}{3} - i\frac{2}{\sqrt{3}}$. Finally, elements of the sequence can be expressed as:

$$x_n = \frac{5}{3} + \left(-\frac{1}{3} + i\frac{2}{\sqrt{3}}\right)\left(-\frac{1}{2} + i\frac{\sqrt{3}}{2}\right)^n + \left(-\frac{1}{3} - i\frac{2}{\sqrt{3}}\right)\left(-\frac{1}{2} - i\frac{\sqrt{3}}{2}\right)^n; \quad n = 0, 1, 2, \ldots.$$

It can be noted that this is not an approximation of elements of the sequence; this expression is exact.

Example 2 (*recurrent roots*). Let us consider a sequence $S = (7, 13, 22, 29, 4, -181, -1010, \ldots)$. $HrS = 3$ because $d^{(3)} = -7 \neq 0$, but

$$d^{(4)} = \begin{vmatrix} 7 & 13 & 22 & 29 \\ 13 & 22 & 29 & 4 \\ 22 & 29 & 4 & -181 \\ 29 & 4 & -181 & -1010 \end{vmatrix} = 0.$$

The characteristic algebraic equation

$$\begin{vmatrix} 7 & 13 & 22 & 29 \\ 13 & 22 & 29 & 4 \\ 22 & 29 & 4 & -181 \\ 1 & \rho & \rho^2 & \rho^3 \end{vmatrix} = -7\rho^3 + 56\rho^2 - 147\rho + 126 = 0$$

yields roots $\rho_1 = 2$; $\rho_2 = \rho_3 = 3$. Then, $n_1 = 1$; $n_2 = 2$ and Eq. (6) takes the following form: $x_n = \mu_{10}\rho_1^n + \mu_{20}\rho_2^n + \mu_{21} n \rho_2^{n-1}$. The linear algebraic system for the identification of coefficients μ_{10}, μ_{20} and μ_{21} reads:

$$\begin{bmatrix} 1 & 1 & 0 \\ \rho_1 & \rho_2 & 1 \\ \rho_1^2 & \rho_2^2 & 2\rho_2 \end{bmatrix} \begin{bmatrix} \mu_{10} \\ \mu_{20} \\ \mu_{21} \end{bmatrix} = \begin{bmatrix} 7 \\ 13 \\ 22 \end{bmatrix}.$$

Solutions are: $\mu_{10} = 7$; $\mu_{20} = 0$; $\mu_{21} = -1$. Thus, finally, $x_n = 7 \cdot 2^n - n \cdot 3^{n-1}$.

Theorem 1. *Let $Hr(x_0, x_1, \ldots) = m < +\infty$ and $x_0, x_1, \ldots \in R$. Then roots ρ_k and coefficients μ_{kl} of the algebraic decomposition of the sequence $\{x_n\}_{n=0}^{+\infty}$ are real or complex conjugate.*

Proof. The algebraic decomposition of the sequence $\{x_n\}_{n=0}^{+\infty}$ is defined by Eq. (6) with $\mu_{k,n_k-1} \neq 0$ and $n_1 + n_2 + \cdots + n_k = m$; $n_1,\ldots,n_k,m \in N$. The equality

$$\mathrm{Im}\left(\sum_{k=1}^{r}\sum_{l=0}^{n_k-1}\mu_{kl}\binom{n}{l}\rho_k^{n-l}\right) = 0$$

holds because $x_0,x_1,\ldots \in R$. On the other hand,

$$\mathrm{Im}\left(\overline{\sum_{k=1}^{r}\sum_{l=0}^{n_k-1}\mu_{kl}\binom{n}{l}\rho_k^{n-l}}\right) = 0$$

holds too (the top line denotes the complex conjugate). But

$$\overline{\sum_{k=1}^{r}\sum_{l=0}^{n_k-1}\mu_{kl}\binom{n}{l}\rho_k^{n-l}} = \sum_{k=1}^{r}\sum_{l=0}^{n_k-1}\overline{\mu_{kl}}\binom{n}{l}(\overline{\rho_k})^{n-l}$$

because $\binom{n}{l} \in R$. But then

$$\mathrm{Im}\left(\sum_{k=1}^{r}\sum_{l=0}^{n_k-1}\mu_{kl}\binom{n}{l}\rho_k^{n-l}\right) = Im\left(\sum_{k=1}^{r}\sum_{l=0}^{n_k-1}\overline{\mu_{kl}}\binom{n}{l}(\overline{\rho_k})^{n-l}\right) = 0; \quad n \in Z_0.$$

The last equality holds if and only one of the following conditions holds true:

(i) μ_{kl}, $\rho_k \in R$;
(ii) μ_{kl}, $\rho_k \in C$ and there exists such $\hat{k}$ that $\rho_{\hat{k}} = \overline{\rho_k}$ and $\mu_{\hat{k}l} = \overline{\mu_{kl}}$ for all $l = 0, 1, \ldots, (n_{\hat{k}} - 1)$; $1 \leqslant k, \hat{k} \leqslant r$; $k \neq \hat{k}$.

End of Proof. □

Theorem 2. *Let $\{x_n\}_{n=0}^{+\infty}$ is a real periodic sequence. Then it is necessary and sufficient that all following statements hold true:*

(i) *A real periodic sequence has a rank; $Hr\{x_n\}_{n=0}^{+\infty} = m$.*
(ii) *All roots of the algebraic decomposition of the sequence are different; $\rho_k \neq \rho_l$; $k \neq l$; $1 \leqslant k,l \leqslant m$.*
(iii) *Modulus of all roots are equal to 1; $|\rho_k| = 1$; $k = 1,2,\ldots,m$.*
(iv) *All ratios $\frac{\arg(\rho_k)}{2\pi}$; $k = 1,2,\ldots,m$ are rational numbers.*

Proof

(i) Since the sequence $\{x_n\}_{n=0}^{+\infty}$ is periodic, there exists such $p \in N$; $m < +\infty$ that $x_{n+p} = x_n$ for all $n \in Z_0$. Then Hankel matrices $H^{(p+k)}$; $k \in N$ contain at least two identical rows and therefore $\det H^{(p+k)} = 0$ for all $k \in N$. Thus, $Hr\{x_n\}_{n=0}^{+\infty} \leqslant p$.
(ii) $\{x_n\}_{n=0}^{+\infty}$ is a periodic sequence and it can be extended into a periodic sequence $\{x_n\}_{n=-\infty}^{+\infty}$. Moreover, there exists such $0 < M < +\infty$ that $|x_n| < M$ for all $n \in Z$ (because $\{x_n\}_{n=-\infty}^{+\infty}$ is a periodic sequence). Let us assume that $Hr\{x_n\}_{n=0}^{+\infty} = m \leqslant p$ and there exist two equal roots: $\rho_{m-1} = \rho_m$, but all other roots are different. Then, according to Eq. (6):

$$x_n = \sum_{k=1}^{m-1}\mu_{k0}\rho_k^n + \mu_{(m-1),1} n \rho_{m-1}^{n-1}; \quad n \in Z; \quad \mu_{(m-1),1} \neq 0. \tag{8}$$

But then there exists such $n_0 \geqslant 0$ that $|x_n| \geqslant M$ for all $|n| \geqslant n_0$, what contradicts to the requirement that $\{x_n\}_{n=0}^{+\infty}$ is a periodic sequence. Analogous contradictions occur when the number of equal roots is higher.

(iii) The proof is analogous to the proof of (ii). Let us assume that $|\rho_k| > 1$; $1 \leqslant k \leqslant m$. Then there exists such $n_0 \geqslant 0$ that $|x_n| \geqslant M$ for all $n \geqslant n_0$. Now, let us assume that $0 < |\rho_k| < 1$; $1 \leqslant k \leqslant m$. Then there exists such $n_0 \geqslant 0$ that $|x_n| \geqslant M$ for all $n \leqslant -n_0$.
(iv) Theorem 1 and statements (i), (ii) and (iii) yield:

$$x_n = \sum_{k=1}^{m}\mu_{k0}\exp(in\varphi_k); \quad n \in Z; \tag{9}$$

where $i^2 = -1$; $\varphi_k = \arg(\rho_k)$; $-\pi \leqslant \varphi_k < \pi$. The sequence $\{x_n\}_{n=0}^{+\infty}$ is periodic if and only $\frac{\varphi_k}{2\pi}$ is a rational number for all $k = 1,2,\ldots m$. Then, Eq. (9) reads:

$$x_n = \sum_{k=1}^{m}\mu_{k0}\exp\left(i2\pi n\frac{a_k}{b_k}\right); \quad n \in Z; \tag{10}$$

where $a_k \in Z$; $b_k \in N$ for all $k = 1,2,\ldots m$. Let p is the least common multiple of $b_1, b_2, \ldots, b_m$; $p \in N$. Then, $\exp\left(i2\pi p \frac{a_k}{b_k}\right) = 1$ for all $k = 1,2,\ldots m$. Thus, p is the period of the sequence: $x_{n+p} = x_n$; $n \in Z$. *End of Proof.* □

Example 3 (the relationship between m and p, Theorem 2, part (ii)). Let us consider a periodic sequence with the period equal to 4. Then, according to Theorem 2, four different roots are: $\rho_1 = 1$; $\rho_2 = -1$; $\rho_3 = i$; $\rho_4 = -i$. Let us construct three different sequences:

(i) $x_n = \mu_{30} \cdot i^n + \mu_{40} \cdot (-i)^n$. The period of this sequence $p = 4$, but $m = Hr\{x_n\}_{n=0}^{+\infty} = 2 \leqslant p$.
(ii) $y_n = \mu_{10} + \mu_{30} \cdot i^n + \mu_{40} \cdot (-i)^n$. The period of this sequence $p = 4$, but $m = Hr\{y_n\}_{n=0}^{+\infty} = 3 \leqslant p$.
(iii) $x_n = \mu_{10} + \mu_{20} \cdot (-1)^n + \mu_{30} \cdot i^n + \mu_{40} \cdot (-i)^n$. The period of this sequence $p = 4$, but $m = Hr\{z_n\}_{n=0}^{+\infty} = 4 \leqslant p$.

3. The computation of ranks of iterative sequences

Logistic map is a paradigmatic model used to illustrate the evolution of a simple nonlinear system to chaos [21]. This discrete dynamical map comprises one control parameter a; we will investigate the interval $0 \leqslant a \leqslant 4$:

$$x_{n+1} = F(x_n) = ax_n(1 - x_n). \tag{11}$$

The algorithm used for the computation of the rank of a sequence S constructed as an iterative solution of the logistic map starting from the initial condition x_0 and at a fixed value of the parameter a is rather straightforward [17]. A sequence of matrices $H^{(m)}$; $m = 2,3,\ldots$ (Eq. (2)) is formed. Theoretically, this process should be continued until such m when $\det\left(H_0^{(m+k)}\right) = 0$ for all $k = 1,2,\ldots$. Unfortunately, as shown before, the rank of a chaotic time series does not exist (m tends to infinity). Therefore we limit the sequence of Hankel matrices setting the upper bound for m. The process is terminated if the sequence of the determinants does not vanish until m reaches the predefined upper bound $\bar{m}$.

Though theoretically one need to find a determinant equal to zero, in practice it suffices to compute determinants up to a certain precision, like the machine epsilon. The computation of determinants is executed until $\left|\det\left(H_0^{(m)}\right)\right| < \varepsilon$ [17]. In this respect such computations do not reveal the rank, but the pseudorank of a sequence (in analogy to the pseudospectrum of a linear operator [22,23]). It is noted in [17] that the upper bound of the rank and the machine epsilon must be preselected individually for each different discrete iterative map. One of the objectives of this paper is to develop an adaptive strategy for the selection of the optimal rank and an optimal value of ε for a concrete sequence S.

First of all we will demonstrate that a higher value of ε may be better (we will define a precise criteria for the comparison) than a lower value of ε (but still higher than the machine epsilon). Let us construct an iterative sequence of the logistic map (Eq. (7)) at $a = 3.59$ starting from $x_0 = 0.5$. Initially, let us fix $\varepsilon = 10^{-10}$ and $\bar{m} = 50$. We construct a sequence of Hankel matrices $\{H^{(k)}\}$ and compute a sequence of determinants $\{d^{(k)}\}$; $k = 2,3,\ldots$ until $|d^{(k)}| < 10^{-10}$ or $k \geqslant 50$. It appears that $|d^{(16)}| < 10^{-10}$. The characteristic algebraic equation Eq. (5) then yields 16 roots; all roots are shown in Fig. 1A (it can be noted that all roots are different). We draw a unit radius circle in the complex plane in Fig. 1A what helps to interpret the modulus of each root.

The base fragment of the sequence is then $(x_0, x_1, x_2, \ldots, x_{29}, x_{30})$. We plot this fragment using a thick black solid line in Fig. 1B. Next we employ Eq. (6) to extrapolate the sequence for 100 steps into the future. The iterated sequence of the logistic map is plotted using a thin black solid line and the extrapolated sequence – a thin red solid line in Fig. 1B. It can be seen that the extrapolated sequence follows the evolution of the logistic map quite well for about 20 steps, but errors start accumulating later.

Analogous numerical experiments are repeated for $\varepsilon = 10^{-19}$ (Fig. 1C, D) and $\varepsilon = 10^{-30}$ (Fig. 1E, F). In order to assess differences between iterated and extrapolates sequences we introduce the measure the extrapolation errors E which is a standard RMSE (root mean square error):

$$E = \sqrt{\frac{1}{100} \sum_{n=2m-1}^{2m+98} (x_n - \tilde{x}_n)^2} \tag{12}$$

where $\tilde{x}_n$ denote elements of the extrapolated sequence. It can be noted that $\tilde{x}_n$ would be equal to x_n for all $n \geqslant 2m - 1$ if ε would be equal to 0.

It is clear that the extrapolation error E depends on ε (Fig. 1). Therefore it is important to identify such ε what would result into a minimal E. The process of minimization of extrapolation errors at $a = 3.59$ and $x_0 = 0.5$ is illustrated in Fig. 2. We perform computations for $\varepsilon = 10^{-k}$; $k = 1,2,\ldots,40$ (Fig. 2A). Extrapolation errors and ranks at different ε are shown in Fig. 2B and C. The minimal value of extrapolation errors is achieved at $k = 19$ and denoted by circles in Fig. 2A, B and C. It can be noted that all further computations are performed using the described technique for the adaptive selection of the optimal value of ε for every particular iterative sequence. This technique can be illustrated by the following algorithm:

(0) Set $\varepsilon = 0.1$.
(i) Set $k = 2$.

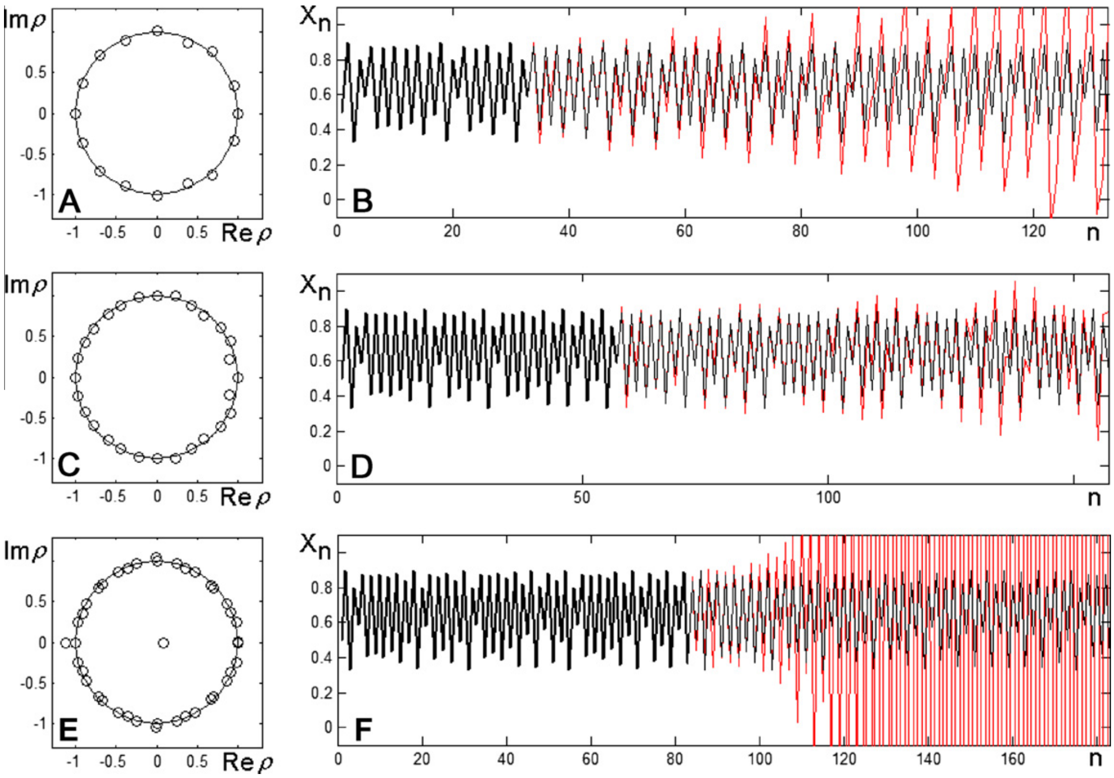

Fig. 1. Algebraic decomposition of transient processes of the logistic map at $a = 3.59$ and $x_0 = 0.5$ at $\varepsilon = 10^{-10}$ (A, B); at $\varepsilon = 10^{-19}$ (C, D) and at $\varepsilon = 10^{-30}$ (E, F). The distribution of roots is shown in A, C and E; transient processes (thin black solid lines), base fragments (thick black solid lines) and extrapolated sequences (thin red lines) are shown in B (*HrS* = 16); D (*HrS* = 28) and F (*HrS* = 41). (For interpretation of the references to colour in this figure legend, the reader is referred to the web version of this article.)

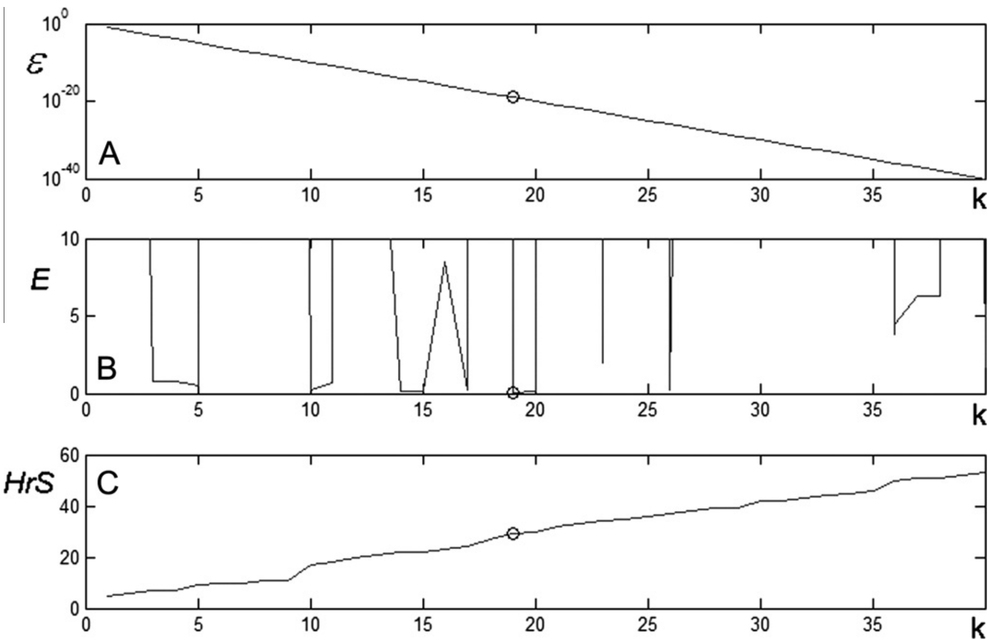

Fig. 2. The minimization of extrapolation errors for the logistic map at $a = 3.59$ and $x_0 = 0.5$. Computations are performed for $\varepsilon = 10^{-k}$; $k = 1,2,\ldots,40$ (A); extrapolation errors are shown in (B); ranks in (C). Minimal extrapolation errors are achieved at $k = 19$ and are denoted by circles.

(ii) Construct the Hankel matrix $H^{(k)}$ and compute $|\det(H^{(k)})|$.
(iii) Check if $|\det(H^{(k)})| < \varepsilon$. If the inequality holds true, compute roots ρ, coefficients μ and the extrapolation error $E(\varepsilon)$ (Eq. (12)) for the current value of k; set $HrS(\varepsilon) = k - 1$. If the inequality does not hold true, set $k = k + 1$ and repeat from step (ii) until the inequality holds true (or k does not exceed the preset upper value).
(iv) Set $\varepsilon = \varepsilon/10$ and repeat from step (i); continue the algorithm until ε does not reach the machine epsilon.
(v) Find the minimal extrapolation error and its index: $[E^*; \varepsilon^*] = \min_{\varepsilon} E(\varepsilon)$. The rank of the best algebraic approximation of the sequence is then equal to $HrS(\varepsilon^*)$.

Note that the number of steps for the computation of the extrapolation error must be preset at the beginning of the algorithm and must be kept constant (the length of the base fragment of the sequence used to reconstruct the algebraic model depends on the current value of k; $k = 100$ is assumed in our experiments). Therefore, the presented algorithm enables the adaptive identification of the best algebraic model for a particular sequence. One of the main advantages of this algorithm is based on the fact that the best algebraic approximation is systematically sought in the parameter plane (ε; k). We avoid the necessity to employ heuristic strategies, ensure the deterministic nature of algorithm and still keep the computational complexity quite low.

4. Numerical experiments with the logistic map

First, the effect of the initial condition to the algebraic decomposition of the solution of the logistic map is demonstrated in Fig. 3. We select the value of the parameter $a = 3.55$ what results into a period-4 attractor after transient processes cease down. Three different initial conditions are selected: $x_0 = 0.01$ (Fig. 3A, B); $x_0 = 0.25$ (Fig. 3B, C) and $x_0 = 0.5$ (Fig. 3E, F). The distribution of roots is shown in Fig. 3A, C and E; transient processes are shown in Fig. 3B, D and F. It can be noted that extrapolations of iterative processes are so good, that no visual differences can be observed between the solution and the extrapolated sequence after 100 steps.

Two-dimensional plots of the rank as a function of the parameter a and the initial condition x_0 are used in [17] in order to reveal the intertwined structure of the stable, the unstable manifold and the manifold of non-asymptotic convergence of the logistic map. Since the primary object of this paper is to explore the onset of chaos using algebraic techniques, we fix one initial condition $x_0 = 0.5$ for all values of the parameter a.

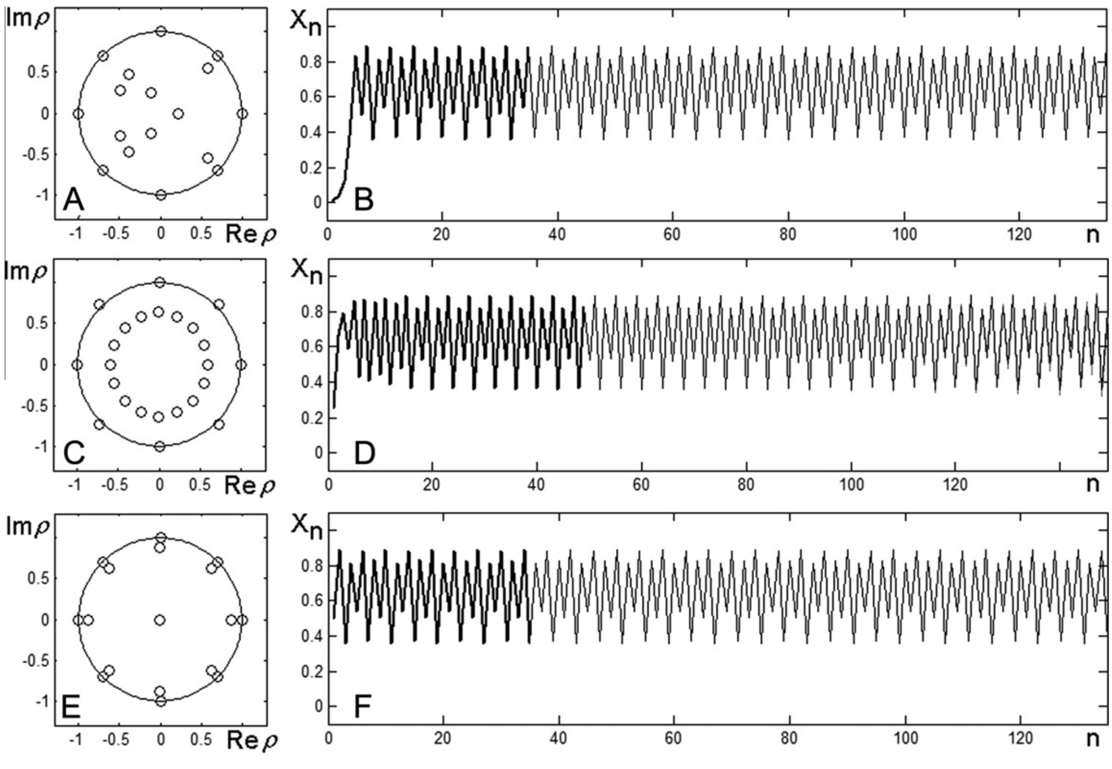

Fig. 3. Algebraic decomposition of transient processes of the logistic map at $a = 3.55$ and $x_0 = 0.01$ (A, B); $x_0 = 0.25$ (C, D) and $x_0 = 0.5$ (E, F). The distribution of roots is shown in A, C and E; transient processes (thin black solid lines), base fragments (thick black solid lines) and extrapolated sequences (thin red lines coincide with thin black lines) are shown in B ($HrS = 17$; $\varepsilon = 10^{-36}$); D ($HrS = 24$; $\varepsilon = 10^{-36}$) and F ($HrS = 17$; $\varepsilon = 10^{-36}$).

Before continuing with the variation of a, we investigate the effect of transient processes to the algebraic decomposition of the solution (Fig. 4). The value of the parameter a is still the same as in the previous experiment; $x_0 = 0.5$. But we now omit first five steps (Fig 4A, B) and first 500 steps (Fig. 4C, D) of the iterative process. The algebraic complexity of the analyzed iterative sequences becomes simpler when initial transient processes are omitted (compare to Fig. 3E, F). Theorem 2 is well illustrated by Fig. 3E, A and C. Roots with modulus lower that 1 gradually dye out when transient processes are omitted. The periodic attractor (the length of the period is 8 iterates) is represented by 8 different roots located on the unit radius circle in the complex plane; all roots are real or complex conjugate. The ratios $\frac{\arg(\rho_k)}{2\pi}$; $k = 1,2,\ldots,8$ read: 0; $\frac{1}{8}$; $\frac{1}{4}$; $\frac{3}{8}$; $\frac{1}{2}$; $-\frac{3}{8}$; $-\frac{1}{4}$ and $-\frac{1}{8}$; the least common multiple of denominators is $p = 8$ what corresponds to the length of the period.

Nevertheless, we explore the onset of chaos without omitting transient processes because first of all it is quite hard to identify at what concrete step a transient process has ceased down, and secondly, the length of transient processes varies with a. Since the object of the investigation is an algebraic approach towards the onset of chaos, we start the iterative process of the logistic map at different values of a ($0 < a < 3.6$), compute the optimal algebraic representation of every iterative process and plot roots in the complex plane for every discrete value of a. We limit computational experiments at $a = 3.6$ because the logistic map approaches the chaotic regime where the algebraic representation can not be useful any more (a chaotic

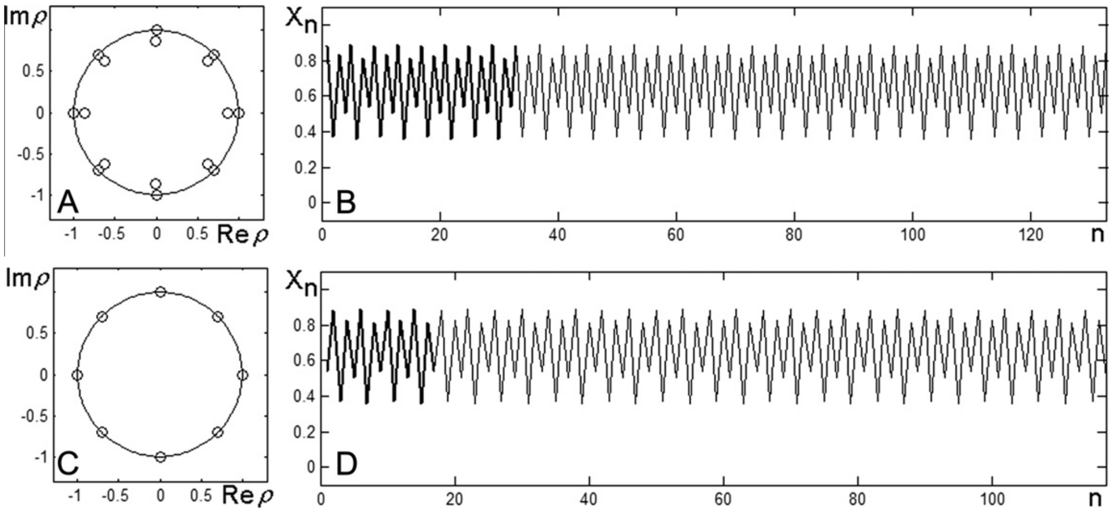

Fig. 4. Algebraic decomposition of iterated sequences produced by the logistic map at $a = 3.55$ and $x_0 = 0.5$ as first 5 steps are omitted (A, B) and first 500 steps are omitted (C, D). The distribution of roots is shown in A and C; transient processes (thin black solid lines), base fragments (thick black solid lines) and extrapolated sequences (thin red lines coincide with thin black lines) are shown in B ($HrS = 16$; $\varepsilon = 10^{-36}$) and D ($HrS = 8$; $\varepsilon = 10^{-36}$).

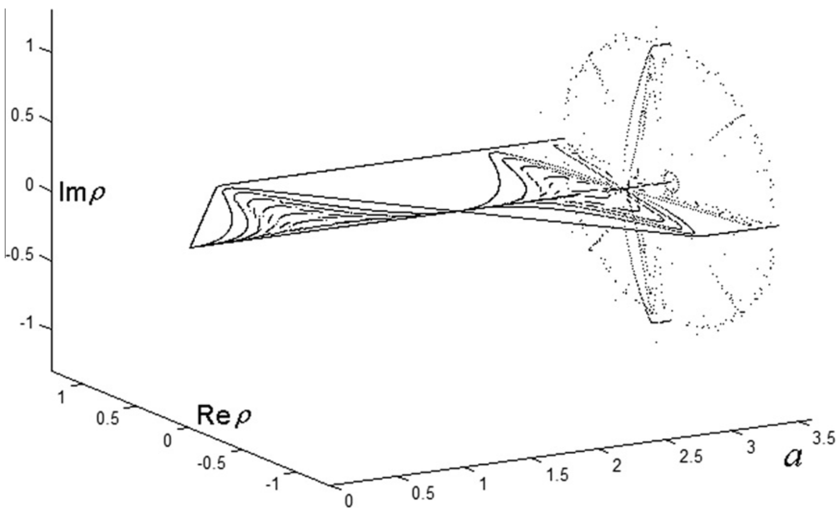

Fig. 5. The distribution of roots of the characteristic algebraic equation for the logistic map in the range $0 < a < 3.6$.

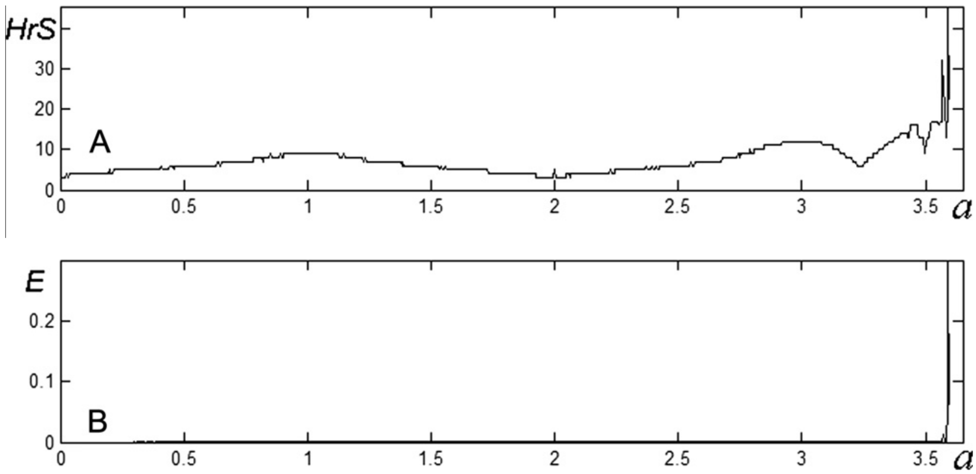

Fig. 6. The variation of the rank of the algebraic representation of the solution of the logistic map (A) and extrapolation errors (B) in the range $0 < a < 3.6$.

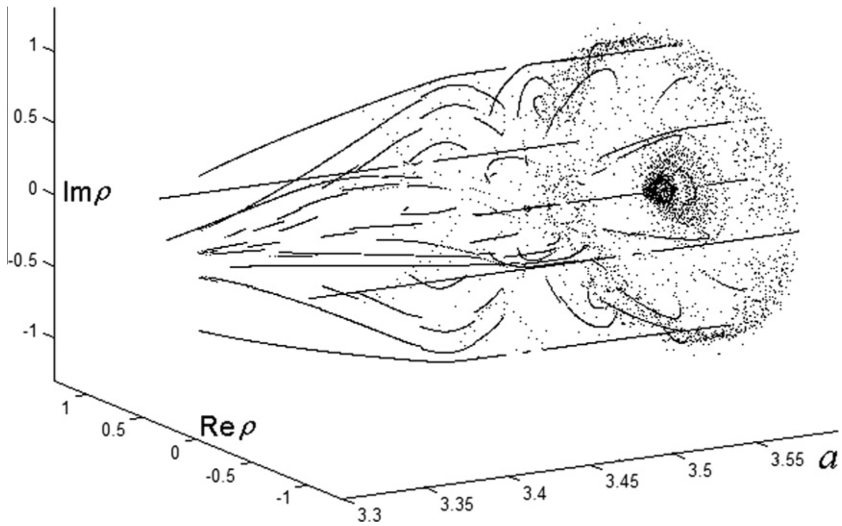

Fig. 7. The distribution of roots of the characteristic algebraic equation for the logistic map in the range $3.3 < a < 3.6$.

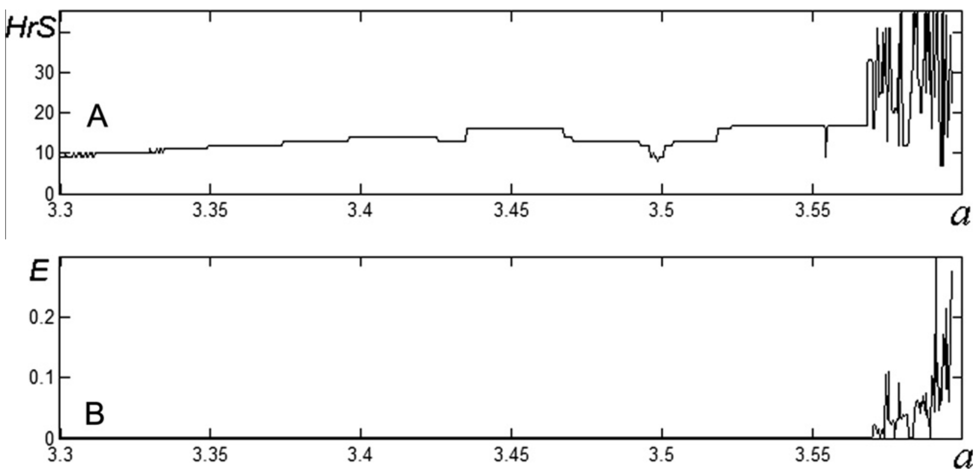

Fig. 8. The variation of the rank of the algebraic representation of the solution of the logistic map (A) and extrapolation errors (B) in the range $3.3 < a < 3.6$.

sequence does not have a rank). The produced 3D image is shown in Fig. 5 (every dot represents a single root of the characteristic algebraic equation).

The evolution of the rank of the algebraic representation of the solution and extrapolation errors is shown in Fig. 6. It is interesting to note that the rank of the solution abruptly jumps over the computational limit (Fig. 6A) as the solution becomes chaotic. Extrapolation errors grow also because an algebraic progression can not represent a chaotic solution (Fig. 6B).

In order to visualize the onset of chaos in more details, we repeat computational experiments and zoon the image of the distribution of roots in the range $3.3 < a < 3.6$ (Fig. 7). One can observe intricate transitions of roots in the complex space until the regular structure of the distribution of roots is lost when the parameter a approaches 3.6. As mentioned previously, Fig. 7 is produced by stepwise incrementing of the parameter a. It is interesting to note that the correlation between the distribution of roots at two consequent discrete values of the parameter a is high until the logistic map does not approach the zone of chaotic solutions. There is no observable correlation left between roots of algebraic representations of solutions at consequent discrete value of the parameter a as the system approaches the chaotic attractor; the variation of the rank and extrapolation errors become unpredictable there also (Fig. 8).

5. Numerical experiments with the Mandelbrot set

We could select another discrete nonlinear dynamic system and explore the onset of chaos using algebraic techniques. Instead we select the discrete Mandelbrot set [24] defined by the following recurrent equality:

$$z_{n+1} = z_n^2 + c; \quad z_0 = 0; \quad (z_n, c) \in C. \tag{13}$$

It is important to note that we are not going to construct the Mandelbrot set, and we are not interested if the iterated sequence stays bounded. We calculate ranks of the iterated sequences instead and plot them in the complex plane (Fig. 9); $\overline{m} = 25$. White zones in Fig. 9 correspond to such values of c where the rank of the generated iterative sequence does not exist.

Since the primary object of this paper is the algebraic approach to the exploration of the onset of chaos, we select the set of discrete sequences on the line $c = s + is$ (the thin solid line in Fig. 9) where $i^2 = -1$; $s \in R$. Discrete iterative sequences in the area near the onset of chaos ($0.32 \leqslant s < 0.35$) are algebraically decomposed using same numerical techniques as described in the previous section; the distribution of roots of characteristic algebraic equations is shown in Fig. 10. The regular structure of the distribution of roots is lost when the parameter c approaches the fractal boundary of the Mandelbrot set. Transient processes become chaotic and the correlation is lost between roots of algebraic representations of recurrent sequences at consequent discrete values of the parameter c.

6. Numerical experiments with real-world time series

So far we have exploited algebraic techniques for the exploration of the onset of chaos in discrete iterative systems. The applicability of the presented algebraic technique for real-world time series remains an important topic of research. The ability to reconstruct the approximating algebraic model of the time series (especially if this series is chaotic and/or contaminated with inevitable noise) would enable the algebraic extrapolation of the time series into the future. The concept of skeleton algebraic sequences is exploited in [25] for the prediction of complex real-world time series. A direct adaptive

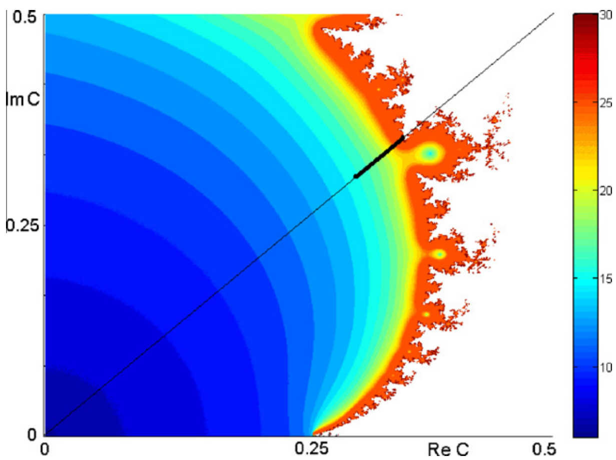

Fig. 9. The distribution of ranks for the Mandelbrot iterative map; the thin solid line represents $c = s + is$.

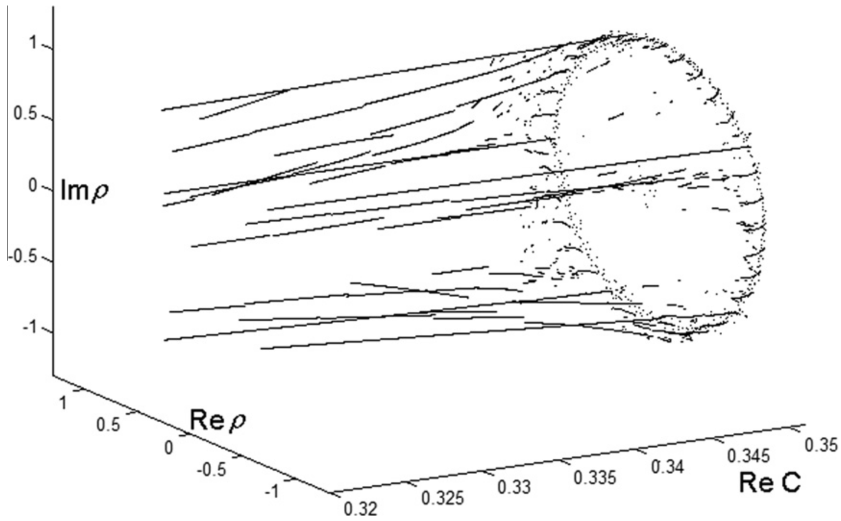

Fig. 10. The distribution of roots of the characteristic algebraic equation for the Mandelbrot iterative map in the range $0.32 \leqslant s < 0.35$; $c = s + is$.

decomposition of the real-world time series into algebraic primitives (using the algorithm presented in section 3) would offer an alternative approach for the construction of an adaptive prediction algorithm.

We select two standard real-world time series: the normalized monthly mean temperatures in southwestern mountain region in a time period started at the year 1932 [26] and the excerpt from normalized daily net retail sales [27]. Fig. 11B shows the best extrapolation (in terms of RMSE) of the normalized monthly mean temperatures in southwestern mountain region for 100 steps into the future; the distribution of roots is shown in Fig. 11A. The best algebraic approximation is reached at $\varepsilon = 10^{-12}$ and $HrS = 21$ what resulted into the extrapolation error $E = 0.245$.

Fig. 11D shows the best algebraic extrapolation of the excerpt from normalized daily net retail sales. Note that this time series is short and that there is not enough data to compute the error of extrapolation for 100 steps into the future. The best approximation is reached at $\varepsilon = 10^{-4}$ and $HrS = 8$ what resulted into the extrapolation error $E = 0.112$.

7. Concluding remarks

The algebraic technique based on Hankel matrices and the rank of a partial solution is proposed for the investigation of the onset of chaos in discrete nonlinear dynamical systems. The distribution of roots of the modified characteristic equation

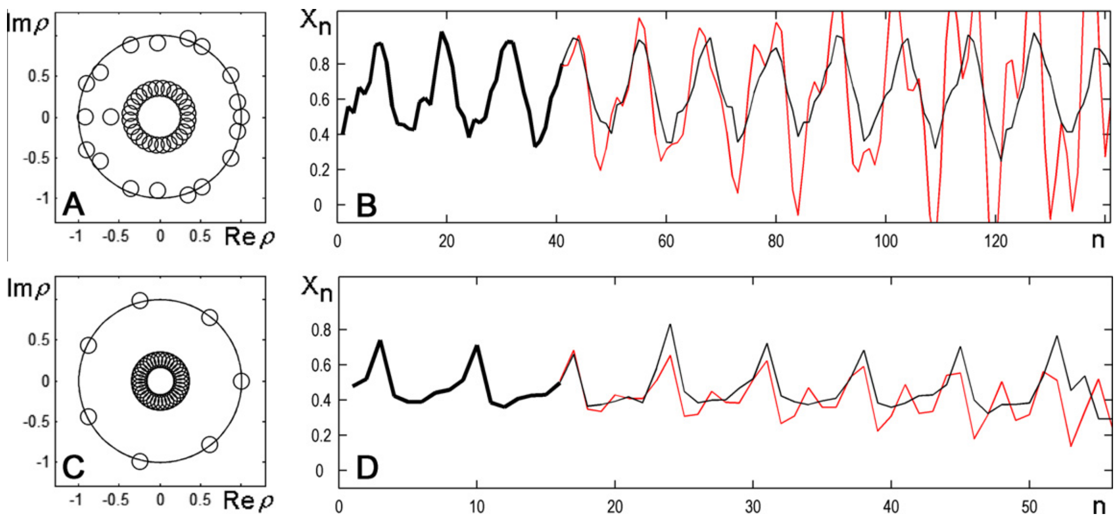

Fig. 11. Algebraic extrapolation of real-world time series: the normalized monthly mean temperatures in southwestern mountain region in a time period started at the year 1932 (A, B) and the excerpt from normalized daily net retail sales (C, D). The distribution of roots is shown in A and C; transient processes (thin black solid lines), base fragments (thick black solid lines) and extrapolated sequences (thin red lines) are shown in B ($HrS = 21$; $\varepsilon = 10^{-12}$) and D ($HrS = 8$; $\varepsilon = 10^{-4}$). (For interpretation of the references to colour in this figure legend, the reader is referred to the web version of this article.)

describes a measure of the complexity of the solution and is used for the characterization of the system's dynamics. The developed technique is applicable for steady-state attractors as well as for transient solutions.

The evolution of the distribution of roots as the system approaches to the chaotic regime reveals interesting properties of the system's dynamics. The inability of a deterministic algebraic technique to decompose a chaotic solution is represented by a computational blow-up of the rank and the stochastic distribution of characteristic roots in the complex plane. Such amplification of the algebraic complexity at the onset of chaos seems to be a universal feature of chaotic nonlinear systems and is demonstrated for two completely different discrete dynamical systems: the logistic map and the Mandelbrot set. Applicability of developed algebraic techniques for the prediction of real-world time series and continuous nonlinear dynamical systems remains an important objective for future research.

References

[1] Feigenbaum MJ. Some formalism and predictions of the period-doubling onset of chaos. North-Holland Math Studies 1982;61:379–94.
[2] Jensen MH. Multifractal scaling structure at the onset of chaos: Theory and experiment. Nucl. Phys B Proc Supplements 1987;2:487–95.
[3] Hale JK, Sternberg N. Onset of chaos in differential delay equations. J Comput Phys 1988;77:221–39.
[4] Brentano P, Zamfir NV. On a measure of the complexity of nuclear states and the onset of chaos. Phys Lett B 1992;297:219–22.
[5] Tennyson J, Farantos SC. Routes to vibrational chaos in triatomic molecules. Chem Phys 1985;93:237–44.
[6] Sung-yool Choi, Eok Kyun Lee. Scaling behavior at the onset of chaos in the logistic map driven by colored noise. Phys Lett A 1995;205:173–8.
[7] Kuznetsov AP, Kuznetsov SP, Sataev IR. A variety of period-doubling universality classes in multi-parameter analysis of transition to chaos. Physica D Nonlinear Phenomena 1997;109:91–112.
[8] Bahar S. Chaotic attractors generated by iterated function systems: 'harmonic decompositions' and the onset of chaos. Chaos Solitons Fract 1997;8:303–12.
[9] Chiarella C. The cobweb model: Its instability and the onset of chaos. Econ Modell 1998;5:377–84.
[10] Robledo A. Universal glassy dynamics at noise-perturbed onset of chaos: a route to ergodicity breakdown. Phys Lett A 2004;328:467–72.
[11] Coraddu M, Lissia M, Tonelli R. Statistical descriptions of nonlinear systems at the onset of chaos. Physica A Statist Mech Appl 2006;365:252–7.
[12] Linage G, Montoya F, Sarmiento A, Showalter K, Parmananda P. Fibonacci order in the period-doubling cascade to chaos. Phys Lett A 2006;359:638–9.
[13] Mocenni C, Facchini A, Vicino A. Comparison of recurrence quantification methods for the analysis of temporal and spatial chaos. Math Comput Modell 2011;53:1535–45.
[14] Lan Y. Cycle expansions: from maps to turbulence. Comm Nonlinear Sci Numer Simulat 2010;15:502–26.
[15] Xin Wu. Is the Hamiltonian geometrical criterion for chaos always reliable? J Geometry Phys 2009;59:1357–62.
[16] Unal A. An algebraic criterion for the onset of chaos in nonlinear dynamical systems. Nonlinear Anal 1989;13:753–65.
[17] Ragulskis M, Navickas Z. The rank of a sequence as an indicator of chaos in discrete nonlinear dynamical systems. Comm Nonlinear Sci Numer Simulat 2011;16:2894–906.
[18] Navickas Z, Bikulciene L. Expressions of solutions of ordinary differential equations by standard functions. Math Modell Anal 2006;11:399–412.
[19] Navickas Z, Ragulskis M, Bikulciene L. Be careful with the Exp function method – additional remarks. Comm Nonlinear Sci Numer Simulat 2010;15:3874–86.
[20] Strogatz S. Nonlinear dynamics and chaos. Adisson Wesley; 1994.
[21] Weisstein EW. Logistic Map. From MathWorld – a Wolfram Web Resource. http://mathworld.wolfram.com/LogisticMap.html.
[22] Trefethen LN. Computation of pseudospectra. Acta Numer 1999;8:247–95.
[23] Trefethen LN. Pseudospectra of linear operators. SIAM Rev 1997;39:383–406.
[24] Weisstein EW. Mandelbrot Set. From MathWorld – A Wolfram Web Resource. http://mathworld.wolfram.com/MandelbrotSet.html.
[25] Ragulskis M, Lukoseviciute K, Navickas Z, Palivonaite R. Short-term time series forecasting based on the identification of skeleton algebraic sequences. Neurocomputing 2011;64:1735–47.
[26] Time Series Data Library by Rob Hyndman; Hydrology. http://robjhyndman.com/TSDL/hydrology/.
[27] Time Series Data Library by Rob Hyndman; Sales. http://robjhyndman.com/TSDL/sales/.